FEBS Open Bio 3 (2013) 291–301

journal homepage: www.elsevier.com/locate/febsopenbio

Beneficial role of overexpression of TFPI-2 on tumour progression in human small cell lung cancer☆

Marion Lavergne[a,b], Marie-Lise Jourdan[e], Claire Blechet[f], Serge Guyetant[b,c,g], Alain Le Pape[a,b,h], Nathalie Heuze-Vourc'h[a,b], Yves Courty[b,c], Stephanie Lerondel[h], Julien Sobilo[h], Sophie Iochmann[a,b,d], Pascale Reverdiau[a,b,d,*]

[a] EA 6305, Université François Rabelais de Tours, Tours F-37032, France
[b] Centre d'Etude des Pathologies Respiratoires, UMR 1100/EA6305, Tours F-37032, France
[c] Inserm UMR 1100, Université François Rabelais de Tours, Tours F-37032, France
[d] IUT de Tours, Université François Rabelais de Tours, Tours F-37082, France
[e] Inserm UMR 1069, Université François Rabelais de Tours, Tours F-37032, France
[f] CHR d'Orléans, Service d'Anatomie pathologique, Orléans F-45067, France
[g] CHRU de Tours, Service d'Anatomie et cytologie pathologiques, Tours F-37044, France
[h] TAAM-UPS44, CIPA, CNRS d'Orléans, Orléans F-45071, France

ARTICLE INFO

Article history:
Received 27 March 2013
Received in revised form 5 June 2013
Accepted 23 June 2013

Keywords:
Tissue factor pathway inhibitor-2
Small cell lung cancer
Metalloproteases
Mouse orthotopic model

ABSTRACT

Tissue factor pathway inhibitor-2 (TFPI-2) is a potent inhibitor of plasmin, a protease which is involved in tumour progression by activating (MMPs). This therefore makes TFPI-2 a potential inhibitor of invasiveness and the development of metastases. In this study, low levels of TFPI-2 expression were found in 65% of patients with small cell lung cancer (SCLC), the most aggressive type of lung cancer. To study the impact of TFPI-2 in tumour progression, TFPI-2 was overexpressed in NCI-H209 SCLC cells which were orthotopically implanted in nude mice. Investigations showed that TFPI-2 inhibited lung tumour growth. Such inhibition could be explained *in vitro* by a decrease in tumour cell viability, blockade of G1/S phase cell cycle transition and an increase in apoptosis shown in NCI-H209 cells expressing TFPI-2. We also demonstrated that TFPI-2 upregulation in NCI-H209 cells decreased MMP expression, particularly by downregulating MMP-1 and MMP-3. Moreover, TFPI-2 inhibited phosphorylation of the MAPK signalling pathway proteins involved in the induction of MMP transcripts, among which MMP-1 was predominant in SCLC tissues and was inversely expressed with TFPI-2 in 35% of cases. These results suggest that downregulation of TFPI-2 expression could favour the development of SCLC.

© 2013 The Authors. Published by Elsevier B.V. on behalf of Federation of European Biochemical Societies. All rights reserved.

1. Introduction

Lung cancer remains the main cause of cancer deaths worldwide [1] and new targeted molecular therapies are currently being developed. Small cell lung cancer (SCLC) is the most common neuroendocrine tumour of the lung (15% of cases) [2,3] and is strongly associated with smoking [4]. It is characterised by tumours that grow rapidly with early metastases to the bones, brain, liver and adrenal glands and therefore a limited number of patients are diagnosed at a local stage. The 5-year survival rate for patients with SCLC is only 2% in advanced stages and 25% for localised disease [5]. Less than 10% of patients with SCLC have a resectable tumour, thus surgical specimens are scarce and most tumour samples come from small biopsies obtained during bronchial endoscopy or mediastinoscopy, which allow diagnosis but do not allow extensive ancillary studies.

Several mechanisms, including degradation of the extracellular matrix (ECM), are involved in the spread of cancer cells from the primary tumour. Among the variety of proteinases acting in proliferation and invasion processes, serine proteinases [6] and matrix metalloproteinases (MMPs) have been shown to be highly expressed and activated in the tumour microenvironment [7], especially in highly aggressive malignant tumours [8]. One potent inhibitor of proteinases is tissue factor pathway inhibitor-2 (TFPI-2), a 32 kDa Kunitz-type serine proteinase inhibitor secreted within the ECM and now considered to be a candidate tumour suppressor gene. In particular, it inhibits plasmin which is involved in MMP activation and could thus regulate ECM degradation and tumour cell invasion. Unfortunately,

☆ This is an open-access article distributed under the terms of the Creative Commons Attribution-NonCommercial-No Derivative Works License, which permits non-commercial use, distribution, and reproduction in any medium, provided the original author and source are credited.

* Corresponding author. Address: Centre d'Etude des Pathologies Respiratoires, Inserm U1100/EA 6305, Faculté de Médecine, 10 Boulevard Tonnellé, 37032 Tours Cedex, France. Tel.: +33 2 47 36 60 67; fax: +33 2 47 36 60 46.
E-mail address: reverdiau@med.univ-tours.fr (P. Reverdiau).

2211-5463/$36.00 © 2013 The Authors. Published by Elsevier B.V. on behalf of Federation of European Biochemical Societies. All rights reserved.
http://dx.doi.org/10.1016/j.fob.2013.06.004

TFPI-2 is downregulated in most aggressive tumours such as glioma [9], non-small cell lung cancer (NSCLC) [10,11], breast cancer [12], melanoma [13], colorectal cancer [14], pancreatic cancer [15] and hepatocellular carcinoma [16]. Such silencing is mainly due to epigenetic changes induced by TFPI-2 promoter hypermethylation and histone deacetylation [12,17,18,19]. Aberrant methylation of TFPI-2 is now being studied to differentiate benign from malign diseases and to evaluate disease progression [20,21,22]. Tumour cells are also able to synthesize an untranslated splice variant of TFPI-2 transcript that correlates with a low level of full-length TFPI-2 transcript [23]. The micro RNA-616 targeting TFPI-2 3'UTR was recently observed in prostate cancer and was found to be inversely correlated with TFPI-2 expression [24]. Moreover, TFPI-2 transcription could be regulated by polymorphisms in the promoter sequence affecting transcription factor binding sites [25]. Absence of TFPI-2 expression can also occur through deletion of the chromosomal region 7q22, as in prostate cancer [26]. We have previously shown that the decrease in TFPI-2 and hypermethylation of its gene promoter in lung cancer were associated with advanced stages of NSCLC, particularly in cases with lymph node metastases [10]. Moreover, methylation of TFPI-2 was also found to be an independent prognostic factor for poor overall survival in patients with NSCLC [11]. More generally, absence or low expression of TFPI-2 in many cancer cells, including lung cancer cells, has been correlated with increase in their invasive potential [27,28,29]. In contrast, induction of TFPI-2 expression using stable transfection or a recombinant adenovirus has been shown to decrease the invasiveness of cancer cells such as prostate cancer cells [30], glioblastoma cells [31], oesophageal carcinoma cells [32] and pancreatic carcinoma cells [33]. No study has yet demonstrated the beneficial role of TFPI-2 restoration in lung cancer, particularly in SCLC.

We therefore investigated TFPI-2 expression in tissue samples from patients with SCLC and evaluated the impact of TFPI-2 restoration in the NCI-H209 cell line on tumour growth in a mouse orthotopic model. In order to explain the role of TFPI-2 in tumour progression, we compared proliferation, cell cycle, apoptosis and MMP expression in NCI-H209 cells expressing TFPI-2 and those without. Finally, we compared immunostaining scores of TFPI-2 and MMP on human SCLC biopsy specimens to evaluate whether downregulation of TFPI-2 might be involved in the aggressiveness of SCLC.

2. Materials and methods

2.1. Human tumour tissue samples

Cases of SCLC were gathered from the files of the Pathology Department of CHRU Tours (France) between February 2004 and March 2007. Tumour diagnosis was performed on biopsy specimens obtained by bronchoscopy ($n = 33$) or mediastinoscopy ($n = 7$) fixed in formalin and paraffin embedded. A total of 40 patients met the following inclusion criteria: histologically confirmed diagnosis of primary SCLC fulfilling the 2004 World Health Organization (WHO) classification criteria, adequate clinical data recorded, tissue specimen available for additional immunohistological assay. The medical records were reviewed to collect the following data: age at diagnosis, sex, smoking history, relevant comorbidities, tumour stage and metastases, date of last consultation or death. Haematoxylin–eosin–safran (HES) and immunohistochemically stained slides were re-examined to confirm the diagnosis according the 2004 the WHO classification of lung tumours. Frozen (−80 °C) tumour material was available for 5 patients who had had a mediastinoscopy. Staging was assessed according to the Veterans' Administration Lung Study Group (VALSG) as recommended by 2004 WHO classification. A statement of 'no objection' was obtained for each patient by complying with French legislation for research.

2.2. Antibodies

The polyclonal rabbit anti-TFPI-2 antibodies were the generous gift of W. Kisiel. Monoclonal rabbit anti-MMP-1 and monoclonal goat anti-MMP-3 antibodies were purchased from R&D systems (Lille, France). Polyclonal rabbit IgG antibody anti-phospho-ERK1/2 and anti-ERK1/2 were purchased from Calbiochem. Monoclonal anti β-actin mouse IgG was from Sigma–Aldrich (Saint-Quentin Fallavier, France). For these antibodies we used peroxidase-labelled anti-mouse IgG (Sigma–Aldrich), peroxidase-labelled anti-goat IgG and anti-rabbit IgG (Santa Cruz, TEBU, Le Perray en Yvelines, France). Monoclonal rabbit IgG antibody against cleaved caspase 3 (Asp175, 5A1E clone), cleaved caspase 9 (Asp330), phospho cRaf (Ser338, 56A6 clone), phospho MEK1/2 (Ser217/221, 41G9 clone) and phospho GSK-3β (Ser9, 5B3 clone) were purchased from Cell Signaling (Ozyme, Saint Quentin en Yvelines, France). Monoclonal mouse IgG1 anti-CDK4 antibody (DCS156 clone), polyclonal rabbit IgG anti-$p15^{INK4B}$ and anti-$p27^{Kip1}$ antibodies were also from Cell Signaling. The secondary antibodies were peroxidase-labelled anti-rabbit IgG and peroxidase-labelled anti-mouse IgG from Cell Signaling. Polyclonal rabbit antibody anti-chromogranin A, monoclonal mouse IgG2 against EMA (clone E29) and IgG1 against cytokeratin (clone KL1) or synaptophysin (clone SY38) were from Dako (Trappes, France). Mouse monoclonal IgG1 anti-CD56 (clone 1B6) was purchased from Novocastra (Leica Microsystèmes SAS, Nanterre, France). Rabbit polyclonal antibodies against MMP-1 and MMP-9, mouse monoclonal IgG1 antibody against MMP-2 (clone A-Gel VC2) and mouse mAb IgG2b against MMP-3 (clone SL-1IID4) were purchased from LabVision Corporation (Thermo Scientific, St Leon-Rot, Germany).

2.3. Cell culture and transfection

The NCI-H209 cell line derived from SCLC was obtained from the ATCC (LGC Promochem, Molsheim, France). Floating aggregate cells were grown in RPMI-1640 medium (Invitrogen, Cergy Pontoise, France) supplemented with 2 mM L-glutamine, 100 IU/mL penicillin, 100 μg/mL streptomycin and 10% endotoxin-free heat-inactivated foetal calf serum (FCS) (Lonza, Basel, Switzerland) at 37 °C in a humidified atmosphere with 5% CO_2. Cells were then transfected with 4 μg of pCMV-luc plasmid (Clontech, Saint Quentin en Yvelines, France) using 10 μg Lipofectamine 2000 reagent according to the manufacturer's instructions (Invitrogen) and as previously described [34]. After transfection, cells were selected in complete medium containing 300 μg/mL G418, and stable clones expressing the highest levels of luciferase (NCI-H209 Luc cells) were isolated and cultured with 50 μg/mL G418 (Invitrogen).

To enhance the tumourigenicity of the NCI-H209 clone selected, two passages were performed *in vivo*. Animals were anaesthetised with 100 mg/kg Ketamine 1000 (Virbac, Wissour, France) and 15 mg/kg Rompun 2% (Bayer Santé, Puteaux, France). NCI-H209 Luc cells (2.5×10^6) in 250 μL of FCS-free RPMI medium containing 4 mg/mL Matrigel™ (Becton Dickinson, Le Pont de Claix, France) were injected into the scapula. Animals were sacrificed after 25 days and the subcutaneous tumours were harvested aseptically, minced into small fragments that were then gently dissociated in the medium. Cells were then cultured in complete medium containing 50 μg/mL G418 until further subcutaneous implantation or transfection.

NCI-H209 Luc cells were transfected with 4 μg of pEF6/V5-His-TOPO plasmid (Invitrogen) containing the TFPI-2 cDNA or only with the plasmid using 10 μg Lipofectamine 2000 reagent (Invitrogen). Six hours after transfection, the medium was replaced by fresh complete medium containing 10% FCS. After 24 h, cells were cultured in 6-well plates with selection medium containing 2 μg/mL blasticidin (InvivoGen, Toulouse, France). Successfully transfected cell clones were then obtained by 3-weeks' culture in the selection medium, and the clones expressing the highest levels of TFPI-2 were selected. TFPI-2

expression was assessed by reverse transcriptase and real-time PCR, Western blotting and immunohistochemical staining.

2.4. Nude mouse orthotopic model of human SCLC

Four-week-old pathogen-free male BALB/c nude mice (Charles River laboratories, Lyon, France) were acclimatised for 2 weeks in a sterile environment before starting the study. All animals were handled and cared for in accordance with National and Institutional guidelines. Protocols were conducted under the supervision of an authorised investigator with the approval of the Institution's Ethics Committee where experiments were performed (CIPA, TAAM-UPS44 Orléans, France). Mice were maintained in sterilised filter-stopped cages throughout the experiments. They were examined daily and monitored for signs of distress, decreased physical activity and weight.

Before implantation, NCI-H209 Luc cells were collected after centrifugation (3 min, 200*g*) and washed twice in FCS-free medium, and the Trypan Blue dye exclusion test was used to assess cell viability >95%. The intrabronchial tumour cell implantation procedure was performed as previously described [34]. Mice were anaesthetised as previously described and the surgery area prepared with skin disinfection using betadine swabs. Immediately before transplantation, a ^{99m}Tc-labelled tin colloid used as tracer was added to the cell suspension containing 4 mg/mL Matrigel™ (Becton Dickinson) and 10 mM EDTA. A 0.5 cm ventral incision was made over the upper region of the trachea to expose the trachea that was punctured using a 23-gauge needle. Cell inoculum (2.5×10^6 tumour cells in 25 μL) was aspirated in a 1.9 Fr x 50 cm blunt-ended catheter (Becton Dickinson) that was inserted and advanced preferentially into the right main bronchus. The position of the catheter was monitored using high resolution radiological imaging (MX-20, Faxitron X-ray Corporation, Wheeling, USA). Tumour cells were slowly injected into the lung and scintigraphic evaluation of cell deposition in the lung was performed (Gamma Imager, Biospace Mesures, Paris, France). The catheter was removed, the incision closed and the animals were placed on a heated pad (37 °C) until fully awake. Animal reactions were observed to ensure recovery from the anaesthesia.

2.5. Bioluminescence imaging

Mice were injected with 100 mg/kg D-luciferin (Promega, Charbonnières, France) and anaesthetised with 2% vapourised isofluorane concentration 4 min later, just before the bioluminescence imaging (BLI). Images were obtained with an IVIS Lumina (Caliper LS, Hopkinton MA, USA) generating a pseudocolour image representing light intensity and superimposed over a greyscale reference image. A mean integration time of 5 min was used for acquisition, and signal intensity was quantified as the sum of all the photons detected from both the ventral and dorsal positions within a region of interest positioned over the lung (Living Image software, v.2.GO, Caliper LS).

2.6. Computed tomography scanning

Microcomputed tomography (CT) was performed on a small animal imager (eXplore Locus, General Electric, Fairfield CT USA) to document tumour location and measurement, mice being anaesthetised with 1.5% isoflurane for the duration of the examination procedure. Source parameters were 80 kV and 450 μA. A total of 360 views were acquired with 1° angle of incrementation, an exposure time of 120 ms and a resolution of 93 μm using external respiratory gating (Biovet, USA). Widths (W, axial), heights (H, mid-sagittal), and lengths (L, mid-sagittal) of tumours were measured and tumour volume was calculated using the ellipsoid formula $4/3\pi$ (W/2 × H/2 × L/2). Three dimensional volume viewing of the lung tumour was performed with eXplore Utilities software/eXplore Reconstruction Utility.

Table 1
Oligonucleotide sequences used for qPCR.

Gene	Sequences (5′3′)
TFPI-2	Forward: AACGCCAACAATTTCTACACCT
	Reverse: TACTTTTCTGTGGACCCCTCAC
MMP-1	Forward: CTGCTGCTGTTCTGGGGT
	Reverse: GCCACTATTTCTCCGCTTTTC
MMP-2	Forward: GGCCCTGTCACTCCTGAGAT
	Reverse: CAGTCCGCCAAATGAACCGG
MMP-3	Forward: ATCCCGAAGTGGAGGAAAAC
	Reverse: GCCTGGAGAATGTGAGTGGA
MMP-9	Forward: AGACCGGTGAGCTGGATAG
	Reverse: GTGATGTTGTGGTGGTGCC
β-Actin	Forward: GCCCTAGACTTCGAGCAAGA
	Reverse: AGGAAGGAAGGCTGAAGAG

2.7. Sacrifice, organ removal and histopathology analysis

Mice were sacrificed by cervical dislocation under anaesthesia. After laparotomy, thoracic and visceral cavities were examined for the presence of metastases, and the lungs and trachea, heart, liver, spleen and brain were collected from each animal. All organs were fixed in 10% buffered formalin, embedded in paraffin and 5-μm thick sections were prepared and stained with HES using a standard procedure.

2.8. Reverse transcription and quantitative polymerase chain reaction (qRT-PCR)

Total mRNA was extracted from 10^6 cells using the Dynabeads mRNA Direct Kit (Invitrogen) according to the manufacturer's instructions. Total mRNA was then reverse transcribed for 1 h at 42 °C in incubation buffer containing 200 μM of each deoxynucleotide triphosphate, 5 μM oligo$(dT)_{20}$, 24 units RNase inhibitor, and 20 units of avian myeloblastosis virus reverse transcriptase (Roche Applied Science, Meylan, France).

The amounts of TFPI-2, MMP-1, -2, -3 and -9 transcripts within cells were assessed by qPCR using the icycler iQ detection system (Bio-Rad, Ivry sur Seine, France). PCR was performed in a total reaction volume of 25 μl containing 2 μl cDNA obtained from mRNA of 2.10^4 cells, 2-fold dilution of Platinum Quantitative PCR SuperMix-UDG (Invitrogen), 0.24 μM of each primer (Eurogentec, Angers, France, Table 1) and a 50,000-fold dilution of Sybr Green solution (Roche Applied Science). To study gene expression, PCR were initiated by decontamination (50 °C for 2 min) and denaturation steps (95 °C for 2 min), followed by *n* cycles (Table 1) at 95 °C for 20 s and at hybridation temperature for 40 s. The melting curve was analysed for each sample to check PCR specificity. β-Actin was used for normalisation of the quantity of RNA, and the C_T value was subtracted from that of the target gene to obtain a ΔC_T value. The relative quantitative measurement of mRNA synthesis was expressed in $2^{|\Delta\Delta CT|}$. The results were then reported to those obtained from a cDNA stock of 852 cells and used as a reference in all experiments.

2.9. Cell preparation, culture supernatant and extracellular matrix isolation

Cells were centrifuged and formalin fixed, and cytoblocks were then prepared for immunohistochemistry analysis. The cytoblock technique was performed with the Shandon kit according to the manufacturer's instructions (Shandon Inc., Pittsburgh, PA). We slightly modified the technique by using only one cytocentrifugation step. The cluster of cells formed was routinely processed and paraffin embedded. Immunohistochemistry was applied to 4 paraffin sections of each specimen.

To prepare surpernatants, cells were grown in fresh medium supplemented with 1% Nutridoma (Roche Applied Science) for 4 days and

were 80-fold concentrated (Microcon, Millipore, Molsheim, France). Proteins from the extracellular matrix were solubilised in TNC buffer (50 mM Tris–HCl pH 7.5, 0.15 M NaCl, 10 mM $CaCl_2$ and 0.05% Brij 35) by agitation and finger flicking for 3 min and then centrifuged at 15,000*g* for 5 min. Proteins from whole cell lysates were extracted and solubilised in RIPA buffer (50 mM Tris–HCl pH 7.5, 0.15 M NaCl, 1 mM EDTA, 1% Igepal® and 0.25% sodium deoxycholate) after agitation between 2 and 10 min incubations at 4 °C and centrifugation at 15,000*g* for 5 min.

2.10. Western blotting

Total protein concentrations of culture supernatants, whole cell lysates and ECM were measured using the Bradford method (Total Protein Kit, Sigma–Aldrich). Proteins (3 μg) were separated on 12% sodium dodecyl sulfate polyacrylamide gel electrophoresis (SDS-PAGE) and transferred onto a nitrocellulose membrane. Membranes were then saturated for 1 h at room temperature in TNT buffer (10 mM Tris–HCl and 150 mM NaCl pH 7.4, 0.1% Tween-20) 1% BSA (Bovine Serum Albumin), incubated overnight at 4 °C with primary antibodies diluted in TNT buffer with 1% BSA and for 1h with appropriate peroxidase-conjugated secondary antibodies after washing with TNT buffer. Following exposure to the Chemiluminescence Reagent Plus (Perkin Elmer Biosystems, Courtaboeuf, France) for 1–10 min, membranes were drained, wrapped in a plastic bag and exposed to autoradiography film (Sigma–Aldrich) for 10 min in the dark.

2.11. Immunohistochemistry analysis

Immunohistochemistry studies were performed on 4 μm formalin-fixed, paraffin-embedded tissue and cytoblock sections. Briefly tissue sections were deparaffinized, rehydratated and subjected to water bath heat antigen retrieval for 20 min in a citrate buffer (Target Retrieval Solution pH 6.0, Dako) for MMP-1, MMP-9, chromogranin A, synaptophysin, CD56, KL1, EMA and TFPI-2, and in an ethylenediamine tetraacetic acid buffer pH 9.0 (Target Retrieval Solution pH 9.0, Dako) for MMP-2 and MMP-3. For all proteins of interest, immunostaining was performed with the Lab Vision Autostainer (Lab Vision Corporation) using a labelled streptavidin-biotin immunoenzymatic detection system with diaminobenzidine as chromogen (UltraVision, Lab Vision Corporation). Slides were haematoxylin counterstained. A semi quantitative intensity scale ranging from 0 to 3 (nil = 0, weak = 1, moderate = 2, strong = 3) was used taking into account both nuclear and cytoplasmic staining.

2.12. Gelatin zymography

MMP-2 and MMP-9 activity in conditioned media and whole cell lysates were determined by gelatin zymography using standard methodology. Briefly, serum-free conditioned and concentrated media or 50 μg proteins were half-diluted in sample buffer and loaded onto 10% (v/v) sodium dodecyl sulfate (SDS) polyacrylamide gels containing 1 mg/ml gelatin (Prolabo, Fontenay-sous-Bois, France). Pro- (92 kDa) and active MMP-9 (82 kDa) as well as pro- (72 kDa) and active MMP-2 (62 kDa) were used as standards (R&D Systems, Lille, France). Electrophoresis was performed at 15 mA/gel constant current for 2 h. Gels were then incubated twice in 100 ml 2.5% (v/v) Triton X-100 (Merck-Eurolab, Fontenay-sous-Bois, France) for 15 min to remove SDS. The Triton solution was then removed and replaced with 100 ml developing buffer (50 mM Tris–HCl, pH 7.5, 5 mM $CaCl_2$, and 0.02% sodium azide). After 16 h incubation at 37 °C, the gels were stained for 3 h in 30% ethanol, 10% acetic acid, and 0.1% Coomassie brilliant blue R-350 (GE Healthcare, Life Technologies, Illkirch, France) and then destained in 45% ethanol and 10% acetic acid. Areas of gelatin digestion were visualised as nonstained regions of the gel, and gels were processed using a GelDoc XR imaging densitometer (Bio-Rad). The intensity of the bands was quantified using Multi-Analyst computer software (Bio-Rad).

2.13. Proliferation assay

Tumour cells (10^5) were seeded in 24-well plates and cultured in culture medium containing 10% FCS. After 1, 4, 7, 12 and 15 days of culture, 140 μL of MTS reagent composed of 3-(4,5-dimethylthiazol-2-yl)-5-(3-carboxymethoxyphenyl)-2H-tetrazolium and an electron coupling agent, phenazine ethosulphate (CellTiter 96® AQ_{ueous}One Solution, Promega, Charbonnières les Bains, France), was added. Cells were incubated for 45 min at 37 °C in a humidified atmosphere containing 5% CO_2 and absorbance was then measured on an ELISA plate reader ($Thermo_{max}$ Molecular Devices, St Grégoire, France) at a wavelength of 490 nm.

2.14. Cell cycle synchronisation and analysis

Cells were seeded (3×10^6 cells) in a 25 cm^2 flask and allowed to grow for 24 h. Synchronisation was then achieved using the method of Barascu et al. [35] and Bugler et al. [36] with slight modifications. Cells were serum-starved for 24 h in RPMI-1640 to produce a G0-G1 cell cycle arrest, then the medium was replaced and cells were incubated in medium containing 2.5 mM thymidin for 16 h, and 300 μM hydroxyurea was added for another 24 h to accumulate the cells at the end of G1. Cells were extensively washed and cell cycle progression allowed once fresh medium containing 10% FCS has been added. Cells were harvested at various time points after being released (from 4 to 60 h), fixed in cold methanol and stored at −20 °C until analysis. After removal of methanol, cells were treated with the Coulter DNA-Prep reagents kit (Beckman Coulter, Villepinte, France) and analysed with a Coulter® Epics XL-MCL™ flow cytometer. Cell cycle distribution was determined with the Multicycle-AV software (Phoenix Flow Systems, San Diego, CA) as previously described [35]. At the time points indicated, cells were also processed for cyclin expression analysis by immunoblotting.

2.15. Apoptosis and caspase 3 and 7 activity in tumour cells and in vivo

Apoptosis was evaluated in tumour cells using a monoclonal antibody against single-stranded DNA to quantitate the apoptotic cells after denaturation of DNA by heating in the presence of formamide. After washing twice with phosphate buffer saline 1 × (PBS), 1.5×10^6 cells/ml were fixed by methanol for 24 h at −20 °C, resuspended in formamide for 5 min at room temperature, heated for 10 min in a water bath at 75 °C and cooled for 15 min in an ice water bath. After centrifugation, cells were incubated with 10 μg/ml anti-ssDNA monoclonal antibody (Mab F7-F26 clone, AbCys, Paris, France) in PBS containing 5% FCS for 15 min at room temperature and rinsed with PBS. Cells were then exposed to fluorescein-conjugated anti-mouse IgM (20 μg/ml in PBS containing 1% non-fat dried milk) for another 15 min at room temperature and rinsed. Negative controls were treated with mouse IgM instead of the specific primary antibody.

The activity of both caspase 3 and 7 was evaluated simultaneously using the ApoTox-Glo™ Triplex assay (Caspase-Glo® 3/7 Substrate, Promega) together with cell viability (GF-AFC Substrate) and cell cytotoxicity (bis-AAF-R110 Substrate). Cells were incubated for 24 h at 37 °C. The substrates GF-AFC and bis-AAF-R110 were added and fluorescence was measured (excitation 400 nm/emission 485 nm and 505 nm/520 nm, respectively) after 30 min incubation at 37 °C. Luminescence was detected after 30 min incubation with the Caspase-Glo® 3/7 Substrate.

Apoptosis in lung cancer cells was also evaluated *in vivo* after subcutaneous implantation of NCI-H209 cells expressing TFPI-2 or non-TFPI-2-expressing cells in nude mice as described above. Animals were sacrificed after 4 weeks and the apoptotic index was determined

together with cleaved caspase 3 immunostaining on formalin-fixed, paraffin-embedded tissue sections using automated BenchMarkXT IHC/ISH staining (Roche) and Fidji software (ONIRIS, Nantes, France). Five microscopic fields were analysed for each sample and the apoptotic index was the positive stained area (pi^2) $\times$ 100 reported to total nuclei (about 500 nuclei). Mitotic index is defined as the number of mitotic cells per field observed at a magnification $\times$ 40.

2.16. Statistical analysis

Data were expressed as means $\pm$ SEM or median $\pm$ 1st quartile/3rd quartile. Statistical analysis was carried out using the Student's *t* test (two tailed) or Mann Whitney test. A *P*-value below or equal to 0.05 was considered statistically significant.

3. Results

3.1. TFPI-2 and MMP expression in human small cell lung cancer

Biopsy specimens of SCLC obtained from 40 patients (30 men and 10 women) aged 45–84 years (median 65 years) were studied. Ninety-seven percent of these patients were smokers. Twenty-five patients (63%) had advanced disease with metastases at the time of diagnosis. Only 2 of 36 patients for whom survival data were available were still alive at the last follow up. The median overall survival was 6 months and the 2-year survival rate was 5.5%. The diagnosis of SCLC was made primarily on haematoxylin–eosin–safran stained slides showing small malignant cells with high mitotic rates. Among the epithelial markers (i.e. pan-cytokeratins (KL1) and epithelial membrane antigen (EMA)) and neuroendocrine differentiation markers (i.e. CD56, chromogranin A and synaptophysin) at least three of them were expressed in all tumours (Fig. 1A). We then examined TFPI-2 and MMP-1, -2, -3 and -9 expression in lung samples of 40 patients with SCLC and established staining intensity from 0 to 3 by immunohistochemistry. Homogeneous expression of TFPI-2 and MMP was observed in 100% of tumour cells in lung samples. Low levels of TFPI-2 (staining intensity of 0 or 1) were found in 26 (65%) SCLC specimens while high levels of TFPI-2 expression were found in only 14 (35%) SCLC specimens, including only 1 with a staining intensity of 3 (Fig. 1B). The highest expression level in MMPs was found for MMP-1 with a staining intensity of 2 for 50% of specimens (Fig. 1C). For MMP-2, MMP-3 and MMP-9, an immunostaining intensity of 1 was predominant in 50%, 57.5% and 61.5% of biopsies, respectively. To determine the relationship between TFPI-2 and MMPs, we compared the immunostaining intensity obtained from the same tissue. In SCLC with low levels of TFPI-2 (0 and 1), MMP staining was mainly equal to that of TFPI-2 or was higher for MMP-1 in only 38% of tissue samples (intensity of 2). In tissues with high levels of TFPI-2 (2 and 3), none had higher levels of MMP staining than those for TFPI-2. Staining levels for MMP-1 were mostly equal to those for TFPI-2, and staining levels lower than those for TFPI-2 were obtained for MMP-2 in all specimens, whereas for MMP-3 and MMP-9 they were lower in 85.7% and 57.1% of tissues, respectively.

3.2. Restoration of TFPI-2 expression in human small cell lung cancer cells

To study the potential involvement of TFPI-2 in the aggressiveness of these lung carcinomas, NCI-H209 cells from a SCLC specimen, positive for all three neuroendocrin markers (chromogranin, synaptophysin and CD56 (Fig. 2A)) were used. These cells were stably transfected to express firefly luciferase and a clone was then passaged twice subcutaneously in mice to enhance tumorogenicity. Cells were then transfected with an empty vector to obtain the 852 control clone or with a plasmid encoding TFPI-2, and the two clones expressing TFPI-2 (T6 and T28) were selected for further experiments.

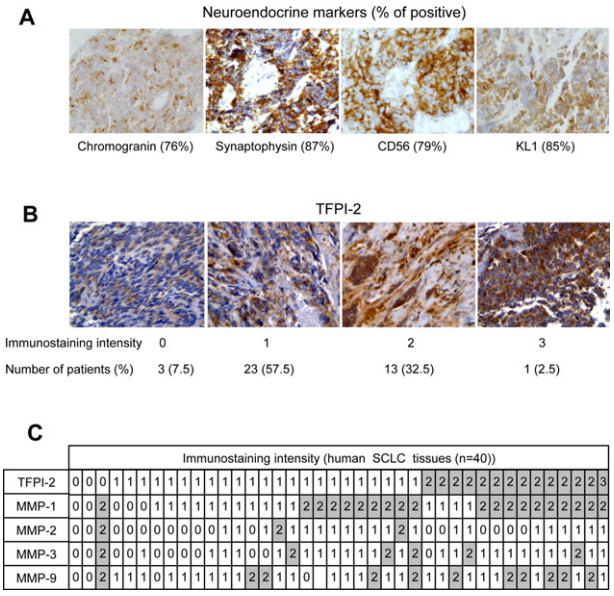

Fig. 1. Immunohistochemistry analysis of small cell lung cancer samples (SCLC). (A) Immunostaining of neuroendocrine and epithelial differentiation markers, chromogranin, synaptophysin, CD56 and KL1 on tissue sections from patients with SCLC. (B) Immunostaining of TFPI-2 using labelled streptavidin–biotin immunoenzymatic detection after incubation with a rabbit polyclonal antibody specific to human TFPI-2 and haematoxylin counterstaining. Representative samples with immunostaining intensity from 0 to 3. Original magnification $\times$ 40. (C) Immunostaining intensity of MMP-1, -2, -3 and -9 according to low (intensity 0 and 1) or high level of TFPI-2 expression (intensity 2 and 3) for each of the 40 tissue samples.

Maximum TFPI-2 level was achieved with the T6 clone as assessed by qPCR (Fig. 2B), the TFPI-2 triplet at 32, 30, and 27 kDa being observed from the extracellular matrix of cells by Western blotting (Fig. 2C) and by immunohistochemistry staining (Fig. 2D). TFPI-2 protein was less strongly expressed in the T28 clone than in the T6 clone although no TFPI-2 was found in 852 cells. These cells exhibited a very low level of TFPI-2 mRNA and a $2^{|\Delta\Delta CT|}$ of 7.75 was obtained when the relative expression of TFPI-2 cDNA from 852 cells was compared to the reference cDNA. Moreover, TFPI-2 mRNA was increased 6,000-fold and 18,000-fold in the T28 and T6 clone respectively compared to 852 cells.

3.3. Up-regulation of TFPI-2 reduced tumour progression in a nude mouse orthotopic model

The impact of TFPI-2 on tumour progression was explored using luciferase-expressing cells intrabronchially implanted in nude mice. Tumour growth was followed by bioluminescence imaging performed every 2 weeks. Of 60 mice, only one died immediately after surgery and two others died of tumour progression. After 9 weeks, lung tumours were obtained in 95% of mice, with slight tracheal bioluminescence in a few animals (5%). In mice implanted with 852 control cells, strong luciferase activity was observed in the lungs from the first measurement performed 3 weeks after implantation to 7 and 9 weeks when the signal remained stable (Fig. 3A). In contrast, mice receiving T6 cells expressing TFPI-2 showed a weak luciferase signal 3 weeks after implantation. This luciferase activity then increased regularly over the experiment but remained significantly lower than in mice receiving 852 cells during 7 weeks. Computed tomography scanning (CT) was performed to document tumour location and volume. In all animals, tumours were located in the lower and middle parts of the lung (Fig. 3B) and a good correlation was demonstrated between bioluminescence and tumour volume measured with CT ($r = 0.87$). Similar results were obtained by measuring lung tumour size with calliper when mice were autopsied at 9 weeks. Histological sections of

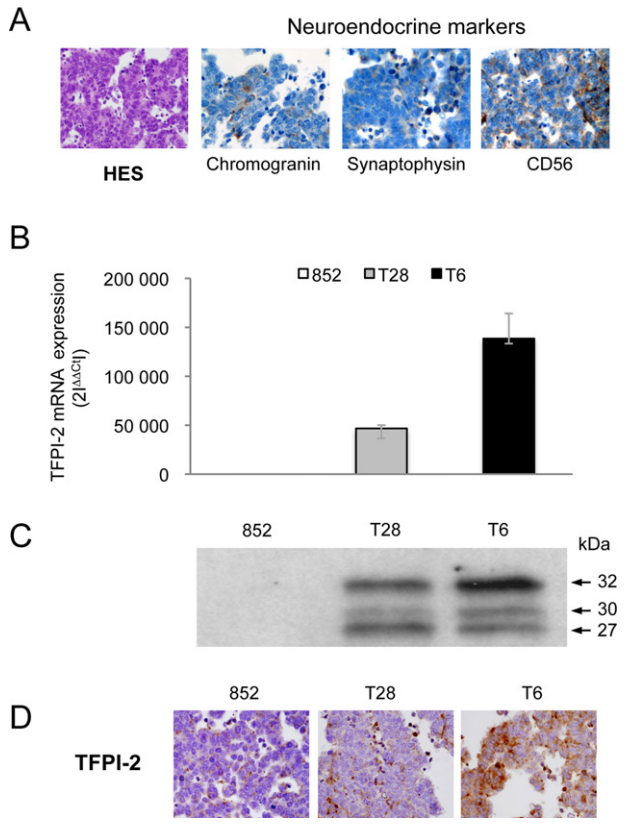

Fig. 2. Development of highly tumorigenic clones of NCI-H209 Luc cells from human SCLC expressing varying amounts of TFPI-2. (A) Immunostaining of the neuroendocrine differentiation markers, chromogranin, synaptophysin and CD56 (original magnification, × 40). (B) Relative quantification of TFPI-2 transcript levels in NCI-H209 Luc cells stably transfected with an empty vector (852) or a plasmid encoding TFPI-2 (T28 and T6) using qRT-PCR. Results expressed in $2^{|\Delta\Delta CT|}$ (β-actin used as control gene) are presented as median ± 1st quartile/3rd quartile from six independent mRNA extractions and qRT-PCR performed in triplicate. (C) TFPI-2 protein expression in ECM extract using a rabbit polyclonal antibody against TFPI-2 by immunoblotting. (D) Immunohistochemistry staining of TFPI-2 (original magnification, × 40).

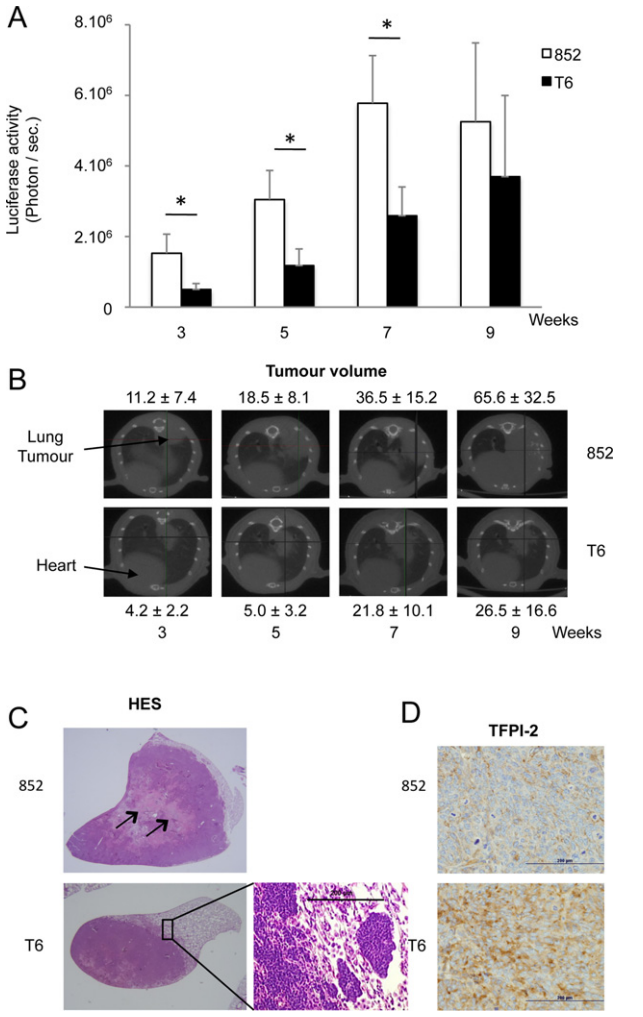

Fig. 3. Longitudinal progression of SCLC in nude mice implanted with NCI-H209 expressing TFPI-2 or not. (A) Cell suspension (2.5 × 10^6 852 or T6 cells) containing 10 mM EDTA and 4 mg/mL Matrigel™ was implanted in the lung. Tumour progression was monitored from 3 to 9 weeks using bioluminescence and a mean of 5 min integration was used for acquisition. Signal intensity was quantified as the sum of all photons detected from both ventral and dorsal positions within the region of interest. Results represent means ± SEM ($n = 30$ animals per group). (B) Tomography scanning of lung tumours was performed to document tumour location and measurement. Axial transverse sections were obtained from 3 to 9 weeks and tumour volumes were calculated using the ellipsoid formula $4/3\pi$ (W/2 × H/2 × L/2). Each scanning image is representative of results obtained in 9 animals per group (mean ± SEM). (C) Histopathology examination (haematoxylin–eosin–saffron staining) was performed on lungs 9 weeks after cell implantation fixed in 10% buffered formalin and embedded in paraffin: 5-μm thick sections (original magnification × 2 and × 40) were used for (D) immunostaining of TFPI-2, (original magnification × 40). Arrows indicate necrotic zones.

lungs stained with HES showed dense tumours with well-delineated borders. The bronchioles were compressed and alveoli invaded and destroyed. Necrotic zones were present in the central region of the tumours, particularly in mice implanted with 852 cells (Fig. 3C), and macrophages were seen in the peripheral region. No metastases were detected after 9 weeks. Immunostaining was also performed on lung tumours at 9 weeks to verify the *in vivo* stability of TFPI-2 expression. As expected, TFPI-2 was highly expressed in lung tumours obtained with cells expressing TFPI-2 (Fig. 3D).

3.4. TFPI-2 reduced tumour cell proliferation and blocked G1/S phase cell cycle transition

To establish whether TFPI-2 could modify the cell proliferation that might influence tumour progression, a MTS assay on cells expressing TFPI-2 and on cells not expressing TFPI-2 was performed every 3 days over a period of 2 weeks. The 3 clones had the same proliferation rate for 10 days (Fig. 4A). In contrast, we clearly demonstrated that TFPI-2 expression in T6 and T28 cells significantly reduced proliferation (4-fold) from the 12th day compared to that of 852 cells.

Cell cycle phase distribution was then monitored by flow cytometry analysis using propidium iodide (Fig. 4B). Although cells were serum starved and treated with thymidin and hydoxyurea, synchronisation was not completely achieved but cells were mostly in the G1 phase (70–80%). At the time of release the 852 cells were more engaged in the cell cycle than cells expressing TFPI-2, as shown by the lowest percentages of cells in the G1 phase and the highest in the S phase. By 16 h a significant blockade in G1 phase was found for T6 and T28 cells (80%) compared to 852 control cells.

Western blotting also showed a marked increase in cyclin-dependent kinase inhibitors p15 and p27 in clones expressing TFPI-2 compared to the control 852 cell line (Fig. 4C). No difference in CDK4 was seen between the 3 clones.

3.5. TFPI-2 increased lung cancer cell apoptosis

To explore further the mechanisms by which TFPI-2 is able to regulate tumour progression, we investigated whether viability, cytotoxicity and particularly apoptosis were affected when this serine protease inhibitor was up-regulated. The three evaluations were performed in the same well for each clone. First, the live-cell protease

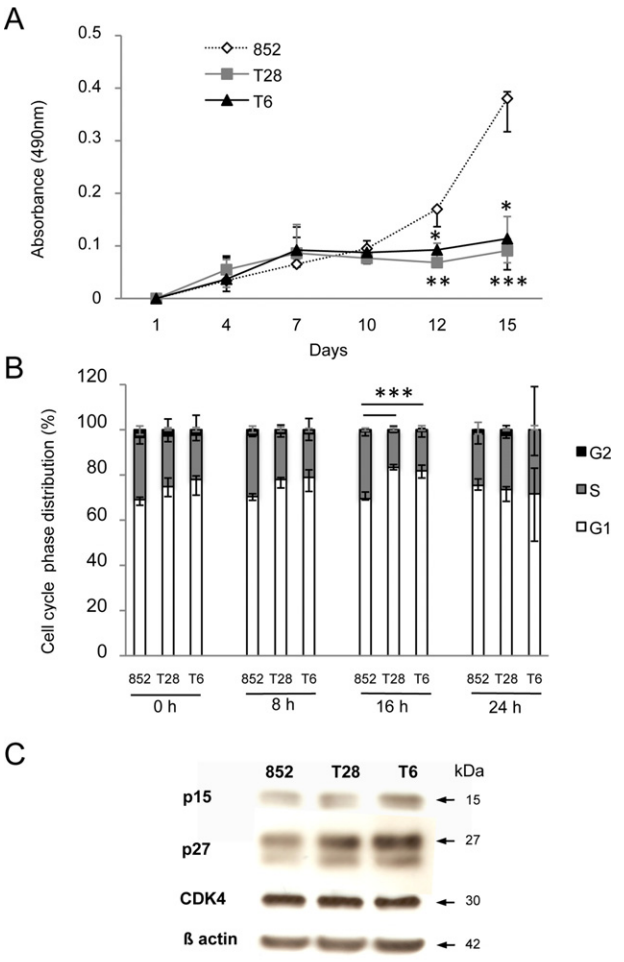

Fig. 4. Impact of TFPI-2 expression on cell growth and cell cycle in NCI-H209 cells. (A) Proliferation of cells expressing TFPI-2 (T6 and T28 cells) or not (852 cells) was assessed by MTS assay every 3 days over 2 weeks. Results represent median and quartile (Q1 and Q3) from at least 4 independent experiments using Mann Whitney statistical analysis with $^{*}p < 0.05$, $^{**}p < 0.01$, $^{***}p < 0.001$. (B) Cell cycle phase distribution of NCI-H209 cells after serum starvation for 8 h, and exposure to 2.5 mM thymidine for 16 h and 300 μM hydroxyurea for 24 h. After culture with medium containing 10% FCS for 0, 8, 16 and 24 h, cells were stained with propidium iodide and analysed by flow cytometry. The percentages of cells in G0/G1, S, G2/M phases are expressed as the median and quartiles of at least 3 independent experiments. (C) Representative immunobloting of p15, p27 and CDK4 involved in cell cycle and β-actin as the loading control, expressed in 852, T28 and T6 cells.

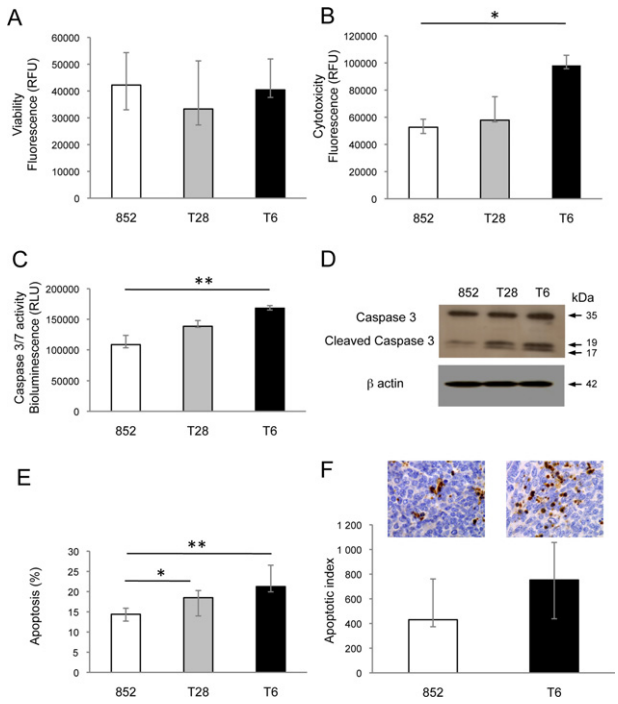

Fig. 5. Effects of TFPI-2 upregulation on cell viability, cytotoxicity and apoptosis. Viability (A) and cytotoxicity (B) of cells expressing TFPI-2 (T6 and T28) or not (852 cells) were simultaneously evaluated using two fluorogenic substrates. Caspase 3 and 7 were evaluated by measuring activity following bioluminescent substrate cleavage (C) and by immunoblotting (D). (E) Apoptosis evaluation of 852, T28 and T6 cells by flow cytometry using a monoclonal antibody against single-stranded DNA. Results represent median and quartiles (Q1 and Q3) from at least 4 independent experiments using Mann Whitney statistical analysis with $^{*}p < 0.05$, $^{**}p < 0.01$, $^{***}p < 0.001$. (F) Apoptosis in 852 and T6 lung cancer cells implanted in nude mice. After immunostaining on lung tissue samples using a cleaved caspase 3 antibody, apoptotic index was defined as the ratio of positive tumour cells to total cells ($n = 500$). Results were obtained in 9 animals per group (median and quartile (Q1 and Q3)).

activity, measured using a fluorogenic substrate cleaved into intact cells, remained unchanged in the 852, T28 and T6 cells (Fig. 5A). In contrast, cytotoxicity was significantly higher in T6 cells expressing TFPI-2, as demonstrated by the addition of a second fluorogenic substrate used simultaneously to measure dead-cell protease activity released from cells that had lost membrane integrity (Fig. 5B). In the second step, apoptosis was also evaluated in the three cell clones by measuring the luminescence signal following caspase-3/7 substrate cleavage. As shown in Fig. 5C, a significant increase in caspase 3/7 activity was found for T6 cells expressing TFPI-2 compared to 852 control cells. Similarly, an increase in cleaved caspase 3 was observed by Western blotting in T28 and T6 cells compared to 852 cells (Fig. 5D). Moreover, apoptotic cells were detected using a monoclonal antibody that specifically recognised single-stranded DNA. An apoptosis level of 15% was observed in 852 cells (Fig. 5E) and a significant increase in apoptotic cells related to the TFPI-2 level expressed in tumour cells was observed. Indeed, more apoptotic cells were obtained with the T6 clone, expressing the highest level of TFPI-2, compared to the T28 clone. Finally, the higher rate of apoptosis in T6 cells was also found *in vivo*. Tumours obtained after subcutaneous implantation of 852 and T6 cells in nude mice for 4 weeks were harvested. After immunostaining for cleaved caspase 3 on sample sections, there was a trend towards higher rate of apoptosis in the T6 cell tumours in-vivo (Fig. 5F). Moreover, a lower mitotic index was observed in mice receiving T6 cells expressing TFPI-2 compared to 852 cells (i.e. 11 vs 23).

3.6. Impact of TFPI-2 over-expression on matrix metalloproteinase expression in SCLC cells

The proteases known to be affected by TFPI-2 expression are matrix metalloproteinases which are involved in ECM degradation and the spread of cancer cells. Levels of MMP-1, -2, -3 and -9 transcripts were therefore quantified in 852, T28 and T6 cells using RT and qPCR (Fig. 6). Varying amounts of MMP transcripts were quantified in all cell clones, except MMP-2 mRNA which was not detected in any of the cell clones studied. A low level of MMP-9 mRNA was expressed in 852 cells and the transcripts decreased in T28 ($p < 0.01$) and T6 cells (Fig. 6A). However, gelatinolytic activity of proMMP-9 and proMMP-2 was found in the conditioned medium of all clones, with a higher signal for proMMP-2. Increased activity was obtained with T28 and T6 clones expressing TFPI-2. In contrast, a decrease in MMP-1 mRNA was found for the two clones expressing TFPI-2, but the difference was significant only for the T6 clone ($p < 0.001$) compared to the 852 control clone (Fig. 6B). Similar results were obtained with MMP-3, as mRNA levels were significantly decreased ($p < 0.01$) in T28 and T6 cells (13-fold and 5-fold, respectively) (Fig. 6C). Western blotting

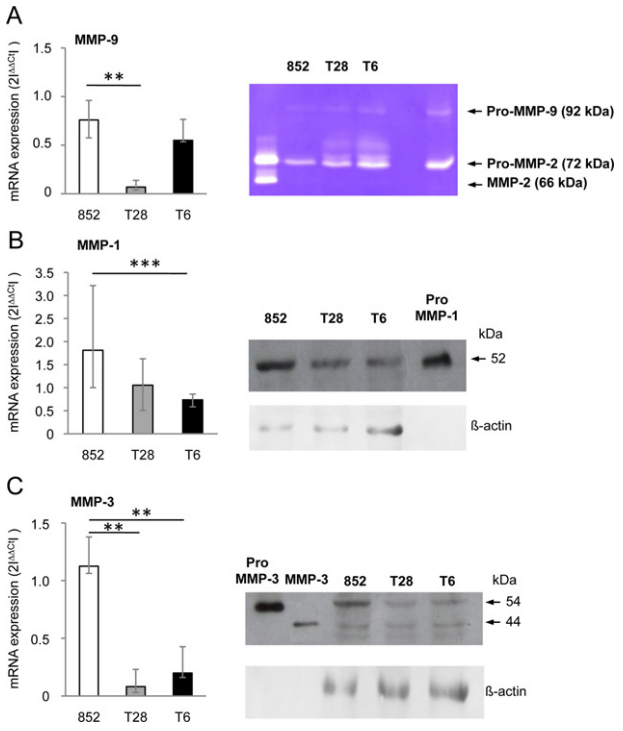

Fig. 6. Impact of TFPI-2 on MMP expression in 852, T28 and T6 cells (A) Relative expression of MMP-9 transcripts normalised to β-actin transcripts using qRT-PCR. Gelatinase activity of MMP-2 and MMP-9 in 80-fold concentrated conditioned media from cells cultured for 4 days and analysed on gelatin zymography. (B) qRT-PCR for MMP-1 transcripts and representative Western blotting analysis of cell lysate proteins extracted from each clone using β-actin as the loading control. (C) qRT-PCR for MMP-3 transcripts and Western blotting analysis of cell lysate proteins. Data for relative quantifications of mRNA represent median and quartiles (Q1 and Q3) from at least 4 independent experiments. Mann Whitney statistical analysis was used to compare results from 852 cells and cells expressing TFPI-2 (T28 and T6 cells) with $^{*}p < 0.05$, $^{**}p < 0.01$, $^{***}p < 0.001$. Western blotting and gelatin zymography are representative of at least 4 independent experiments.

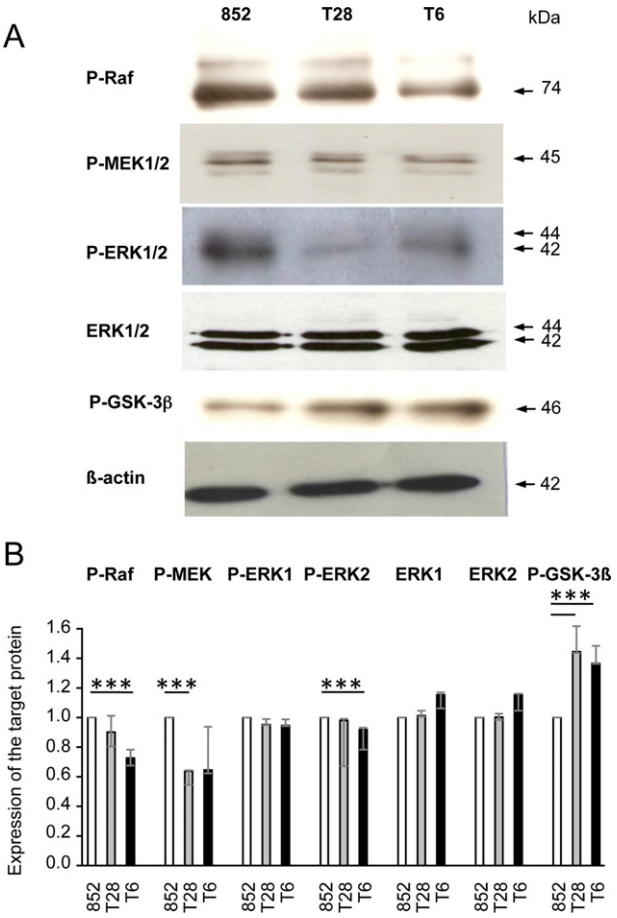

Fig. 7. TFPI-2 effects on phosphorylation state of proteins involved in MAPK signalling pathway. (A) Representative Western blotting of P-Raf, P-MEK, P-ERK, ERK, P-GSK-3β and β-actin as control with 852, T28 and T6 cell lysate extracts. (B) Densitometric analysis of immunoblots. The relative intensity of target protein is normalised to β-actin and then reported to 852 cell values. Data represent the median and quartiles Q1 and Q3 of three immunoblots. Mann Whitney statistical analysis was used to compare results from 852 cells and cells expressing TFPI-2 (T28 and T6 cells) with $^{*}p < 0.05$, $^{**}p < 0.01$, $^{***}p < 0.001$.

also clearly showed that this decrease in MMP-1 and MMP-3 transcripts was associated with lower protein expression (Fig. 6B and C). The proform of MMP-1 at 52 kDa was observed, while MMP-3 was visualised as both pro and active forms in the 3 clones (54 and 44 kDa, respectively).

3.7. TFPI-2 inhibited phosphorylation of proteins involved in MAPK signalling pathway

To determine whether the MAPK signalling pathway which is involved in the induction of MMP synthesis was activated in TFPI-2-upregulated small cell lung cancer cells, we investigated phosphorylation of RAF, MEK1/2 and ERK1/2 proteins using immunoblotting. As shown in Fig. 7, overexpression of TFPI-2 in T28 and T6 clones decreased the level of P-RAF, P-MEK1/2 and P-ERK-2, but the difference was significant only for one clone expressing TFPI-2. No difference was obtained in ERK-1/2 and P-ERK-1 between the three clones. In contrast, serine-9 phosphorylation of GSK3β was significantly enhanced in T28 and T6 cells. No difference in protein loading was shown by β-actin immunodetection.

4. Discussion

TFPI-2 is a tumour suppressor gene which is often downregulated in particularly aggressive tumours such as gliomas [9,37], melanomas [13], hepatocellular carcinomas [16] and non-small cell lung cancer [10]. However, documentation for SCLC, the most aggressive lung cancer, is poor due to the scarcity of specimens available to study the mechanisms of tumour progression. The originality of the study presented here was the investigation of TFPI-2 expression in lung samples from patients with SCLC. For the first time we demonstrated low levels of expression of TFPI-2 in 65% of tumours, most patients being diagnosed at an advanced stage of the cancer. Indeed, extremely poor survival was observed, with a median overall survival of 6 months and a 2-year survival rate of 5.5%. Such TFPI-2 downregulation may be due to promoter methylation, as shown in various types of cancer [12,14,16,18,37,38] and particularly in patients with later stages of NSCLC, as we have previously reported [10]. Moreover, in a previous study, poor prognosis was associated with TFPI-2 promoter methylation status in NSCLC [11], suggesting that the methylation of the TFPI-2 gene or TFPI-2 expression might be independent factors for poor survival or favourable outcome, respectively. However, the impact of TFPI-2 expression levels in SCLC cells that themselves exhibit low level of TFPI-2 has not yet been established. We therefore investigated whether the TFPI-2 restoration in the NCI-H209 cell line might have a beneficial effect by regulating mechanisms involved in tumour progression. The NCI-H209 SCLC cell line was established from bone marrow metastases of a patient with histologically confirmed small cell lung carcinoma [39]. These cells are small in size with scant cytoplasm, and show the classic neuroendocrine features and markers of SCLC [40] and grow as packed floating cell aggregates, irregular in outline. Moreover, genome sequencing of NCI-H209 cells recently

identified the combined loss of RB1 and TP53 typically observed in SCLC, demonstrating that this cell line clearly represents this disease [41,42]. Using this cell line, that we previously genetically modified to express firefly luciferase, we developed a reproducible and reliable nude mouse orthotopic model that resembles human SCLC [34]. The growth of the primary tumour was sensitively and non-invasively followed by bioluminescence imaging that allowed real-time monitoring of tumour progression in the same animals over a 2- to 9-week period without sacrificing animals at different tumour stages. Using this original lung cancer model with cells transfected to overexpress TFPI-2, our results demonstrated that TFPI-2 expression significantly inhibited lung tumour growth over 7 weeks after implantation compared to tumour growth measured with cells expressing very low levels of TFPI-2. With the latter cells we also observed necrotic zones in the central region of the tumours, as frequently reported in human SCLC [40]. After 7 weeks, no significant difference was found between tumours obtained with cells with or without TFPI-2 expression. When necrosis was present, light emission generated by oxidation of luciferase substrate was decreased due to ATP depletion, thus underestimating cancer cell counts. We therefore combined 2D bioluminescence and tomography scanning that clearly demonstrated that tumour volume developed with cells not expressing TFPI-2 was greater than when TFPI-2 was present. Few studies have been performed in mice for other kinds of human cancers and these have shown that TFPI-2 expression limits tumour progression. Indeed, restoration of TFPI-2 expression in fibrosarcoma cells after transfection with a plasmid encoding TFPI-2 has been reported to reduce subcutaneous tumour growth [43] and similar results were obtained in an orthotopic pancreatic carcinoma model [33].

Several mechanisms are involved in tumour progression, including cell proliferation and apoptosis, cell migration and invasion requiring degradation of the extracellular matrix by a variety of proteinases such as metalloproteinases. A decrease in cancer cell proliferation after TFPI-2 expression has also been reported in pancreatic carcinoma cells [15,33], oesophageal and nasopharyngeal cancer cells [18], gallblader carcinoma cells [44], glioma cells [45] and choriocarcinoma cells [46]. Nevertheless, this effect may be tumour-specific, as some authors have attributed no antiproliferative effect to TFPI-2 [29,32]. Indeed, in contrast to NSCLC where TFPI-2 did not impact cell on proliferation [27], we showed in our study that TFPI-2 reduced the cell proliferation rate, with a low overall number of cells expressing TFPI-2. We also demonstrated for the first time in SCLC that TFPI-2 blocks the G1/S transition phase of the cell cycle, associated with an increase in the cyclin-dependent kinase inhibitors p15 and p27. The involvement of p27 (that blocks G1/S-transition by regulating CDK2 [47]) in cell cycle dysregulation has been reported by several authors [48,49] in NSCLC as well as in other cancers such as prostate cancer [50] and fibrosarcoma [51]. Moreover, transduction of NSCLC cells with an adenovirus expressing p27 was found to result in G1/S arrest and induce suppression of xenograft lung tumour growth in nude mice [52]. Low levels of p27 in lung cancer have also been reported to be associated with poor prognosis [53,54], and a better survival rate was reported in NSCLC when p27 expression was high [55]. However, these findings are controversial [56] and could be explained by a dual effect of p27 depending on its nuclear sequestration, thus becoming non-functional in inhibiting cell cycle progression. We also showed that the p15 cell cycle regulator which increased in cells expressing TFPI-2 might also be involved in the inhibition of proliferation observed in these cells. Indeed, increases in p15 and p27 expression were also obtained concomitantly with inhibition of proliferation and induction of arrest of the G1 phase cell-cycle in a A549 lung cancer cell line treated with a derivative of genistein [57]. Interestingly, genistein has been reported to induce TFPI-2 and to inhibit growth and metastasis of breast cancer cells [58]. Although the p15 gene promoter was less frequently deleted or aberrantly methylated in lung cancers than in other cancers [59,60], the overall survival of patients with promoter methylation was shortened in NSCLC [61].

In parallel of the limited proliferation of lung cancer cells expressing TFPI-2, we also demonstrated induction of apoptosis in these cells via an increase in caspase 3 activity both *in vitro* and *in vivo*. These findings are in agreement with previous studies demonstrating the pro-apoptotic activity of TFPI-2. TFPI-2 is thus able to induce death receptor-mediated apoptosis through increases in FasL, TNF-α, and death domains FADD and TRADD. It also induces apoptosis through the mitochondrial-dependent caspase cascade, with upregulation of pro-apoptotic Bax, cleaved Caspase 3 and 9, released cytochrom c and Apaf-1 and a decrease in anti-apoptotic Bcl2 [31,62,63]. Moreover, we have shown here that TFPI-2 could also regulate apoptosis by inhibiting GSK-3β (glycogen synthase kinase-3β) activity via Ser-9 phosphorylation, as observed in SCLC cells expressing TFPI-2. GSK-3β is involved in both glycogen metabolism and cell signalling and can regulate cell cycle progression and apoptosis, with consequently pro or anti tumour activity [64]. Indeed, GSK-3β activity is enhanced by phosphorylation of tyrosine 216 and inhibited by phosphorylation of serine 9. It has been shown that GSK3 inhibition can decrease viability and induce apoptosis in colon cancer cells [65], glioma cells [66], and pancreatic cancer cells [67]. Moreover, GSK-3 inhibition suppresses NF-κB, downregulates anti-apoptotic protein Bcl2 and induces cleaved caspase-3 following exposure of pancreatic cancer cells to TRAIL [68]. In the present study, we also showed with a subcutaneous xenograft model that more apoptotic cells and fewer cells undergoing mitosis were observed in tumours developed with cells expressing TFPI-2. Similar results have also been reported in mice that received fibrosarcoma cells expressing TFPI-2, with higher percentages of cells undergoing apoptosis in the core cell region of tumours [43].

Cell invasion and tumour progression also require degradation of the extracellular matrix by several proteinases, particularly metalloproteinases. Several authors have described TFPI-2 as an inhibitor of MMP activity directly or mainly for MMP-1, -2, -3 and -9 via plasmin inhibition [32,69,70]. In addition to these direct mechanisms of inhibition, our *in vitro* findings demonstrated a decrease in MMP-1 and MMP-3 transcripts and proteins in SCLC cells expressing TFPI-2 that could also explain the inhibition of tumour growth observed in mice. In accordance with our previous study, when TFPI-2 expression was silenced in NSCLC cells, we observed increases in MMP-1 and MMP-3 transcript levels and proteins [27]. These findings therefore suggest that TFPI-2 may regulate MMP mRNA expression like a transcription factor and this could be due to its carboxy-terminal tail that is internalised into cells and translocated into the nucleus [71]. On the other hand, the decreases in MMP-1 and -3 may be explained by downregulation of the mitogen-activated protein kinase (MAPK) pathway involving Ras/Raf/MAPK/extracellular signal-regulated kinase (ERK), as observed in glioma cells [72]. Indeed, we demonstrated in the present study that cells expressing TFPI-2 tend to reduce phosphorylation of Raf and MEK that are known to be involved in the activation of many MMP [73]. Moreover, the down-regulation of the ERK signalling pathway has been reported to be involved in the inhibition of lung tumour cell invasion [74]. Surprisingly, MMP-2, -3 and -9 were slightly expressed in lung samples without relationship with high or low levels of TFPI-2. The low level of MMP-2 and MMP-9 detected in human SCLC tissues could explain that conditioned media need to be concentrated about 80-fold to detect these pro-MMP in 852 cells. In fact, we previously observed in TFPI-2 silenced NCI-H460 a decrease in MMP-2 mRNA that was inversely correlated to MMP-1 and -3 expression [27]. Moreover when MMP-2 and -9 mRNA was assessed in tumour and non-affected tissues from patients with NSCLC, we showed a similar level of MMP-2 mRNA in both tissues whereas MMP-1, -3 and -9 mRNA were significantly higher in tumours ([25] and personal data). This could be explained by a difference in localisation of MMP-2 detected in stromal cells while MMP-9 was mainly detected in tumour cells. Some authors showed that MMP-2 located

in stromal cells rather than in tumour cells plays a significant role in the prognosis of NSCLC [75]. In contrast, we found that MMP-1 was predominant in SCLC tissues. Moreover, TFPI-2 expression was the inverse of MMP-1 in 35% of cases and thus was in accordance with our *in vitro* studies. Because surgical specimens of SCLC are scarce, our study was performed mainly on small samples obtained by bronchial endoscopy or mediastinoscopy, thus allowing only immunohistochemistry analyses. The impact of TFPI-2 on MMP expression remains to be further explored within other SCLC tissues.

In conclusion, the study we report provides evidence that TFPI-2 can inhibit SCLC tumour progression by inhibiting cell proliferation mainly by the induction of apoptosis and also arresting the transition phase G1/S cell cycle. Moreover, TFPI-2 might limit tumour invasion by a mechanism dependent on regulation of MMP-1 and -3 and the ERK signalling pathway. The frequent downregulation of TFPI-2 in SCLC probably contributes to the aggressive nature of this lung cancer.

Acknowledgements

We are grateful to Walter Kisiel (Department of Pathology, University of New Mexico, Health Sciences Center, Albuquerque, NM, USA) for kindly providing the anti-TFPI-2 rabbit polyclonal antibody. We thank Didier Grenêche and Laurent Mahé for their contribution to the iconography. We also particularly thank Maryline Le Mée, Stéphanie Rétif, Sophie Hamard, the staff of the Pathology Departments of Tours and Orléans Hospitals, Laëtitia Dorso and Jérôme Abadie from Oniris in Nantes for excellent technical assistance and Doreen Raine for editing the English text. This study was supported by the 'Ligue Contre le Cancer', and we especially thank the Departmental committees of Charente, Maine et Loire, Indre et Deux-Sèvres and also the 'Région Centre' (THERICAPT project).

References

[1] Siegel, R., Naishadham, D. and Jemal, A. (2012) Cancer statistics, 2012. CA Cancer J. Clin. 62(1), 10–29.
[2] Sutherland, K.D. and Berns, A. (2010) Cell of origin of lung cancer. Mol. Oncol. 4(5), 397–403.
[3] Travis, W.D. (2010) Advances in neuroendocrine lung tumors. Ann Oncol 21(Suppl. 7), vii65–vii71.
[4] Lee, P.N., Forey, B.A. and Coombs, K.J. (2012) Systematic review with meta-analysis of the epidemiological evidence in the 1900s relating smoking to lung cancer. BMC Cancer 12, 385.
[5] Planchard, D. and Le Pechoux, C. (2011) Small cell lung cancer, new clinical recommendations and current status of biomarker assessment. Eur. J. Cancer 47(Suppl. 3), S272–S283.
[6] Nathalie, H.V., Chris, P., Serge, G., Catherine, C., Benjamin, B., Claire, B. et al. (2009) High kallikrein-related peptidase 6 in non-small cell lung cancer cells, an indicator of tumour proliferation and poor prognosis. J. Cell. Mol. Med. 13(9B), 4014–4022.
[7] Stamenkovic, I. (2003) Extracellular matrix remodelling, the role of matrix metalloproteinases. J. Pathol. 200(4), 448–464.
[8] Noel, A., Jost, M. and Maquoi, E. (2008) Matrix metalloproteinases at cancer tumor–host interface. Semin. Cell. Dev. Biol. 19(1), 52–60.
[9] Rao, C.N., Lakka, S.S., Kin, Y., Konduri, S.D., Fuller, G.N., Mohanam, S. et al. (2001) Expression of tissue factor pathway inhibitor 2 inversely correlates during the progression of human gliomas. Clin. Cancer Res. 7(3), 570–576.
[10] Rollin, J., Iochmann, S., Blechet, C., Hube, F., Regina, S., Guyetant, S. et al. (2005) Expression and methylation status of tissue factor pathway inhibitor-2 gene in non-small-cell lung cancer. Br. J. Cancer 92(4), 775–783.
[11] Wu, D., Xiong, L., Wu, S., Jiang, M., Lian, G. and Wang, M. (2012) TFPI-2 methylation predicts poor prognosis in non-small cell lung cancer. Lung Cancer 76(1), 106–111.
[12] Guo, H., Lin, Y., Zhang, H., Liu, J., Zhang, N., Li, Y. et al. (2007) Tissue factor pathway inhibitor-2 was repressed by CpG hypermethylation through inhibition of KLF6 binding in highly invasive breast cancer cells. BMC Mol. Biol. 8, 110.
[13] Nobeyama, Y., Okochi-Takada, E., Furuta, J., Miyagi, Y., Kikuchi, K., Yamamoto, A. et al. (2007) Silencing of tissue factor pathway inhibitor-2 gene in malignant melanomas. Int. J. Cancer 121(2), 301–307.
[14] Hibi, K., Goto, T., Kitamura, Y.H., Sakuraba, K., Shirahata, A., Mizukami, H. et al. (2010) Methylation of TFPI2 gene is frequently detected in advanced well-differentiated colorectal cancer. Anticancer Res. 30(4), 1205–1207.
[15] Sato, N., Parker, A.R., Fukushima, N., Miyagi, Y., Iacobuzio-Donahue, C.A., Eshleman, J.R. et al. (2005) Epigenetic inactivation of TFPI-2 as a common mechanism associated with growth and invasion of pancreatic ductal adenocarcinoma. Oncogene 24(5), 850–858.
[16] Wong, C.M., Ng, Y.L., Lee, J.M., Wong, C.C., Cheung, O.F., Chan, C.Y. et al. (2007) Tissue factor pathway inhibitor-2 as a frequently silenced tumor suppressor gene in hepatocellular carcinoma. Hepatology 45(5), 1129–1138.
[17] Hube, F., Reverdiau, P., Iochmann, S., Cherpi-Antar, C. and Gruel, Y. (2003) Characterization and functional analysis of TFPI-2 gene promoter in a human choriocarcinoma cell line. Thromb. Res. 109(4), 207–215.
[18] Jia, Y., Yang, Y., Brock, M.V., Cao, B., Zhan, Q., Li, Y. et al. (2012) Methylation of TFPI-2 is an early event of esophageal carcinogenesis. Epigenomics 4(2), 135–146.
[19] Takada, H., Wakabayashi, N., Dohi, O., Yasui, K., Sakakura, C., Mitsufuji, S. et al. (2010) Tissue factor pathway inhibitor 2 (TFPI2) is frequently silenced by aberrant promoter hypermethylation in gastric cancer. Cancer Genet. Cytogenet. 197(1), 16–24.
[20] Glockner, S.C., Dhir, M., Yi, J.M., McGarvey, K.E., Van Neste, L., Louwagie, J. et al. (2009) Methylation of TFPI2 in stool DNA, a potential novel biomarker for the detection of colorectal cancer. Cancer Res. 69(11), 4691–4699.
[21] Kisiel, J.B., Yab, T.C., Taylor, W.R., Chari, S.T., Petersen, G.M., Mahoney, D.W. et al. (2011) Stool DNA testing for the detection of pancreatic cancer, assessment of methylation marker candidates. Cancer 118(10), 2623–26231.
[22] Ohtsubo, K., Watanabe, H., Okada, G., Tsuchiyama, T., Mouri, H., Yamaguchi, Y. et al. (2008) A case of pancreatic cancer with formation of a mass mimicking alcoholic or autoimmune pancreatitis in a young man. Possibility of diagnosis by hypermethylation of pure pancreatic juice. JOP 9(1), 37–45.
[23] Kempaiah, P., Chand, H.S. and Kisiel, W. (2007) Identification of a human TFPI-2 splice variant that is upregulated in human tumor tissues. Mol. Cancer 6, 20.
[24] Ma, S., Chan, Y.P., Kwan, P.S., Lee, T.K., Yan, M., Tang, K.H. et al. (2011) MicroRNA-616 induces androgen-independent growth of prostate cancer cells by suppressing expression of tissue factor pathway inhibitor TFPI-2. Cancer Res. 71(2), 583–592.
[25] Rollin, J., Regina, S., Vourc'h, P., Iochmann, S., Blechet, C., Reverdiau, P. et al. (2007) Influence of MMP-2 and MMP-9 promoter polymorphisms on gene expression and clinical outcome of non-small cell lung cancer. Lung Cancer 56(2), 273–280.
[26] Dong, J.T. (2001) Chromosomal deletions and tumor suppressor genes in prostate cancer. Cancer Metastasis Rev. 20(3–4), 173–193.
[27] Gaud, G., Iochmann, S., Guillon-Munos, A., Brillet, B., Petiot, S., Seigneuret, F. et al. (2011) TFPI-2 silencing increases tumour progression and promotes metalloproteinase 1 and 3 induction through tumour–stromal cell interactions. J. Cell. Mol. Med. 15(2), 196–208.
[28] Iochmann, S., Blechet, C., Chabot, V., Saulnier, A., Amini, A., Gaud, G. et al. (2009) Transient RNA silencing of tissue factor pathway inhibitor-2 modulates lung cancer cell invasion. Clin. Exp. Metastasis 26(5), 457–467.
[29] Lakka, S.S., Konduri, S.D., Mohanam, S., Nicolson, G.L. and Rao, J.S. (2000) In vitro modulation of human lung cancer cell line invasiveness by antisense cDNA of tissue factor pathway inhibitor-2. Clin. Exp. Metastasis 18(3), 239–244.
[30] Konduri, S.D., Tasiou, A., Chandrasekar, N. and Rao, J.S. (2001) Overexpression of tissue factor pathway inhibitor-2 (TFPI-2), decreases the invasiveness of prostate cancer cells in vitro. Int. J. Oncol. 18(1), 127–131.
[31] George, J., Gondi, C.S., Dinh, D.H., Gujrati, M. and Rao, J.S. (2007) Restoration of tissue factor pathway inhibitor-2 in a human glioblastoma cell line triggers caspase-mediated pathway and apoptosis. Clin. Cancer Res. 13(12), 3507–3517.
[32] Ran, Y., Pan, J., Hu, H., Zhou, Z., Sun, L., Peng, L. et al. (2009) A novel role for tissue factor pathway inhibitor-2 in the therapy of human esophageal carcinoma. Hum. Gene Ther. 20(1), 41–49.
[33] Tang, Z., Geng, G., Huang, Q., Xu, G., Hu, H., Chen, J. et al. (2011) Expression of tissue factor pathway inhibitor 2 in human pancreatic carcinoma and its effect on tumor growth, invasion, and migration in vitro and in vivo. J. Surg. Res. 167(1), 62–69.
[34] Iochmann, S., Lerondel, S., Blechet, C., Lavergne, M., Pesnel, S., Sobilo, J. et al. (2012) Monitoring of tumour progression using bioluminescence imaging and computed tomography scanning in a nude mouse orthotopic model of human small cell lung cancer. Lung Cancer 77(1), 70–76.
[35] Barascu, A., Besson, P., Le Floch, O., Bougnoux, P. and Jourdan, M.L. (2006) CDK1-cyclin B1 mediates the inhibition of proliferation induced by omega-3 fatty acids in MDA-MB-231 breast cancer cells. Int. J. Biochem. Cell Biol 38(2), 196–208.
[36] Bugler, B., Schmitt, E., Aressy, B. and Ducommun, B. (2010) Unscheduled expression of CDC25B in S-phase leads to replicative stress and DNA damage. Mol. Cancer 9, 29.
[37] Vaitkiene, P., Skiriute, D., Skauminas, K. and Tamasauskas, A. (2012) Associations between TFPI-2 methylation and poor prognosis in glioblastomas. Medicina (Kaunas) 48(7), 345–349.
[38] Hube, F., Reverdiau, P., Iochmann, S., Rollin, J., Cherpi-Antar, C. and Gruel, Y. (2003) Transcriptional silencing of the TFPI-2 gene by promoter hypermethylation in choriocarcinoma cells. Biol. Chem. 384(7), 1029–1034.
[39] Gazdar, A.F., Carney, D.N., Nau, M.M. and Minna, J.D. (1985) Characterization of variant subclasses of cell lines derived from small cell lung cancer having distinctive biochemical, morphological, and growth properties. Cancer Res. 45(6), 2924–2930.
[40] Travis, W.D. (2012) Update on small cell carcinoma and its differentiation from squamous cell carcinoma and other non-small cell carcinomas. Mod. Pathol. 25(Suppl. 1), S18–S30.
[41] Kitamura, H., Yazawa, T., Sato, H., Okudela, K. and Shimoyamada, H. (2009) Small cell lung cancer, significance of RB alterations and TTF-1 expression in its carcinogenesis, phenotype, and biology. Endocr. Pathol. 20(2), 101–107.
[42] Pleasance, E.D., Stephens, P.J., O'Meara, S., McBride, D.J., Meynert, A., Jones, D.

et al. (2010) A small-cell lung cancer genome with complex signatures of tobacco exposure. Nature 463(7278), 184–190.
[43] Chand, H.S., Du, X., Ma, D., Inzunza, H.D., Kamei, S., Foster, D. et al. (2004) The effect of human tissue factor pathway inhibitor-2 on the growth and metastasis of fibrosarcoma tumors in athymic mice. Blood 103(3), 1069–1077.
[44] Qin, Y., Zhang, S., Gong, W., Li, J., Jia, J. and Quan, Z. (2012) Adenovirus-mediated gene transfer of tissue factor pathway inhibitor-2 inhibits gallbladder carcinoma growth in vitro and in vivo. Cancer Sci 103(4), 723–730.
[45] Gessler, F., Voss, V., Seifert, V., Gerlach, R. and Kogel, D. (2011) Knockdown of TFPI-2 promotes migration and invasion of glioma cells. Neurosci. Lett. 497(1), 49–54.
[46] Zhou, Q., Xiong, Y., Chen, Y., Du, Y., Zhang, J., Mu, J. et al. (2012) Effects of tissue factor pathway inhibitor-2 expression on biological behavior of BeWo and JEG-3 cell lines. Clin. Appl. Thromb. Hemost. 18(5), 526–533.
[47] Chu, I.M., Hengst, L. and Slingerland, J.M. (2008) The Cdk inhibitor p27 in human cancer, prognostic potential and relevance to anticancer therapy. Nat. Rev. Cancer 8(4), 253–267.
[48] Li, H., Sun, L., Tang, Z., Fu, L., Xu, Y., Li, Z. et al. (2012) Overexpression of TRIM24 correlates with tumor progression in non-small cell lung cancer. PLoS One 7(5), e37657.
[49] Ling, Y.H., Li, T., Yuan, Z., Haigentz, M. Jr., Weber, T.K. and Perez-Soler, R. (2007) Erlotinib, an effective epidermal growth factor receptor tyrosine kinase inhibitor, induces p27KIP1 up-regulation and nuclear translocation in association with cell growth inhibition and G1/S phase arrest in human non-small-cell lung cancer cell lines. Mol. Pharmacol. 72(2), 248–258.
[50] Wang, C.D., Huang, J.G., Gao, X., Li, Y., Zhou, S.Y., Yan, X. et al. (2011) Fangchinoline induced G1/S arrest by modulating expression of p27, PCNA, and cyclin D in human prostate carcinoma cancer PC3 cells and tumor xenograft. Biosci. Biotechnol. Biochem. 74(3), 488–493.
[51] Matsui, T.A., Murata, H., Sowa, Y., Sakabe, T., Koto, K., Horie, N. et al. (2010) A novel MEK1/2 inhibitor induces G1/S cell cycle arrest in human fibrosarcoma cells. Oncol. Rep. 24(2), 329–333.
[52] Park, K.H., Seol, J.Y., Yoo, C.G., Kim, Y.W., Han, S.K., Lee, E.H. et al. (2001) Adenovirus expressing p27(Kip1) induces growth arrest of lung cancer cell lines and suppresses the growth of established lung cancer xenografts. Lung Cancer 31(2–3), 149–155.
[53] Esposito, V., Baldi, A., De Luca, A., Groger, A.M., Loda, M., Giordano, G.G. et al. (1997) Prognostic role of the cyclin-dependent kinase inhibitor p27 in non-small cell lung cancer. Cancer Res. 57(16), 3381–3385.
[54] Ishihara, S., Minato, K., Hoshino, H., Saito, R., Hara, F., Nakajima, T. et al. (1999) The cyclin-dependent kinase inhibitor p27 as a prognostic factor in advanced non-small cell lung cancer, its immunohistochemical evaluation using biopsy specimens. Lung Cancer 26(3), 187–194.
[55] Zhuang, Y., Yin, H.T., Yin, X.L., Wang, J. and Zhang, D.P. (2011) High p27 expression is associated with a better prognosis in East Asian non-small cell lung cancer patients. Clin. Chim. Acta 412(23–24), 2228–2231.
[56] Sterlacci, W., Fiegl, M., Hilbe, W., Jamnig, H., Oberaigner, W., Schmid, T. et al. (2010) Deregulation of p27 and cyclin D1/D3 control over mitosis is associated with unfavorable prognosis in non-small cell lung cancer, as determined in 405 operated patients. J. Thorac. Oncol 5(9), 1325–1336.
[57] Peng, B., Cao, J., Yi, S., Wang, C., Zheng, G. and He, Z. (2013) Inhibition of proliferation and induction of G(1)-phase cell-cycle arrest by dFMGEN, a novel genistein derivative, in lung carcinoma A549 cells. Drug Chem. Toxicol. 39(2), 196–204.
[58] Lee, W.Y., Huang, S.C., Tzeng, C.C., Chang, T.L. and Hsu, K.F. (2007) Alterations of metastasis-related genes identified using an oligonucleotide microarray of genistein-treated HCC1395 breast cancer cells. Nutr. Cancer 58(2), 239–246.
[59] Chaussade, L., Eymin, B., Brambilla, E. and Gazzeri, S. (2001) Expression of p15 and p15.5 products in neuroendocrine lung tumours, relationship with p15(INK4b) methylation status. Oncogene 20(45), 6587–6596.
[60] Jha, A.K., Nikbakht, M., Jain, V., Capalash, N. and Kaur, J. (2012) p16(INK4a) and p15(INK4b) gene promoter methylation in cervical cancer patients. Oncol. Lett. 3(6), 1331–1335.
[61] Kurakawa, E., Shimamoto, T., Utsumi, K., Hirano, T., Kato, H. and Ohyashiki, K. (2001) Hypermethylation of p16(INK4a) and p15(INK4b) genes in non-small cell lung cancer. Int. J. Oncol. 19(2), 277–281.
[62] Kempaiah, P. and Kisiel, W. (2008) Human tissue factor pathway inhibitor-2 induces caspase-mediated apoptosis in a human fibrosarcoma cell line. Apoptosis 13(5), 702–715.
[63] Tasiou, A., Konduri, S.D., Yanamandra, N., Dinh, D.H., Olivero, W.C., Gujrati, M. et al. (2001) A novel role of tissue factor pathway inhibitor-2 in apoptosis of malignant human gliomas. Int. J. Oncol 19(3), 591–597.
[64] Jacobs, K.M., Bhave, S.R., Ferraro, D.J., Jaboin, J.J., Hallahan, D.E. and Thotala, D. (2012) GSK-3beta, A bifunctional role in cell death pathways. Int. J. Cell Biol, 930710.
[65] Shakoori, A., Mai, W., Miyashita, K., Yasumoto, K., Takahashi, Y., Ooi, A. et al. (2007) Inhibition of GSK-3 beta activity attenuates proliferation of human colon cancer cells in rodents. Cancer Sci 98(9), 1388–1393.
[66] Kotliarova, S., Pastorino, S., Kovell, L.C., Kotliarov, Y., Song, H., Zhang, W. et al. (2008) Glycogen synthase kinase-3 inhibition induces glioma cell death through c-MYC, nuclear factor-kappaB, and glucose regulation. Cancer Res. 68(16), 6643–6651.
[67] Marchand, B., Tremblay, I., Cagnol, S. and Boucher, M.J. (2012) Inhibition of glycogen synthase kinase-3 activity triggers an apoptotic response in pancreatic cancer cells through JNK-dependent mechanisms. Carcinogenesis 33(3), 529–537.
[68] Mamaghani, S., Simpson, C.D., Cao, P.M., Cheung, M., Chow, S., Bandarchi, B. et al. (2012) Glycogen synthase kinase-3 inhibition sensitizes pancreatic cancer cells to TRAIL-induced apoptosis. PLoS One 7(7), e41102.
[69] Herman, M.P., Sukhova, G.K., Kisiel, W., Foster, D., Kehry, M.R., Libby, P. et al. (2001) Tissue factor pathway inhibitor-2 is a novel inhibitor of matrix metalloproteinases with implications for atherosclerosis. J. Clin. Invest 107(9), 1117–1126.
[70] Rao, C.N., Mohanam, S., Puppala, A. and Rao, J.S. (1999) Regulation of ProMMP-1 and ProMMP-3 activation by tissue factor pathway inhibitor-2/matrix-associated serine protease inhibitor. Biochem. Biophys. Res. Commun 255(1), 94–98.
[71] Kempaiah, P., Chand, H.S. and Kisiel, W. (2009) Human tissue factor pathway inhibitor-2 is internalized by cells and translocated to the nucleus by the importin system. Arch. Biochem. Biophys 482(1–2), 58–65.
[72] Kunapuli, P., Kasyapa, C.S., Hawthorn, L. and Cowell, J.K. (2004) LGI1, a putative tumor metastasis suppressor gene, controls in vitro invasiveness and expression of matrix metalloproteinases in glioma cells through the ERK1/2 pathway. J. Biol. Chem. 279(22), 23151–23157.
[73] Huntington, J.T., Shields, J.M., Der, C.J., Wyatt, C.A., Benbow, U., Slingluff, C.L. Jr. et al. (2004) Overexpression of collagenase 1 (MMP-1) is mediated by the ERK pathway in invasive melanoma cells, role of BRAF mutation and fibroblast growth factor signaling. J. Biol. Chem. 279(32), 33168–33176.
[74] Shih, Y.W., Shieh, J.M., Wu, P.F., Lee, Y.C., Chen, Y.Z. and Chiang, T.A. (2009) Alpha-tomatine inactivates PI3K/Akt and ERK signaling pathways in human lung adenocarcinoma A549 cells, effect on metastasis. Food Chem. Toxicol. 47(8), 1985–1995.
[75] Ishikawa, S., Takenaka, K., Yanagihara, K., Miyahara, R., Kawano, Y., Otake, Y. et al. (2004) Matrix metalloproteinase 2 status in stromal fibroblasts, not in tumor cells, is a significant prognostic factor in non-small-cell lung cancer. Clin. Cancer Res. 10, 6579–6585.